

## RESEARCH ARTICLE

# Developmental malformations resulting from high-dose maternal tamoxifen exposure in the mouse

Miranda R. Sun<sup>☉</sup>, Austin C. Steward<sup>☉</sup>, Emma A. Sweet<sup>☉</sup>, Alexander A. Martin, Robert J. Lipinski<sup>☉</sup>\*

Department of Comparative Biosciences, School of Veterinary Medicine, University of Wisconsin-Madison, Madison, WI, United States of America

☉ These authors contributed equally to this work.

\* [robert.lipinski@wisc.edu](mailto:robert.lipinski@wisc.edu)



## OPEN ACCESS

**Citation:** Sun MR, Steward AC, Sweet EA, Martin AA, Lipinski RJ (2021) Developmental malformations resulting from high-dose maternal tamoxifen exposure in the mouse. PLoS ONE 16(8): e0256299. <https://doi.org/10.1371/journal.pone.0256299>

**Editor:** Christiana Ruhrberg, University College London, UNITED KINGDOM

**Received:** April 9, 2021

**Accepted:** August 3, 2021

**Published:** August 17, 2021

**Copyright:** © 2021 Sun et al. This is an open access article distributed under the terms of the [Creative Commons Attribution License](https://creativecommons.org/licenses/by/4.0/), which permits unrestricted use, distribution, and reproduction in any medium, provided the original author and source are credited.

**Data Availability Statement:** All relevant data are within the manuscript and its [Supporting Information](#) files.

**Funding:** This study was supported by The University of Wisconsin Office of Vice Chancellor for Graduate and Research Education Fall Competition Award (<https://research.wisc.edu/funding/fall-competition/>) to RJL and The NIH Office of the Director NIH Training Grant (T35OD011078) to EAS. The funders had no role in

## Abstract

Tamoxifen is an estrogen receptor (ER) ligand with widespread use in clinical and basic research settings. Beyond its application in treating ER-positive cancer, tamoxifen has been co-opted into a powerful approach for temporal-specific genetic alteration. The use of tamoxifen-inducible Cre-recombinase mouse models to examine genetic, molecular, and cellular mechanisms of development and disease is now prevalent in biomedical research. Understanding off-target effects of tamoxifen will inform its use in both clinical and basic research applications. Here, we show that prenatal tamoxifen exposure can cause structural birth defects in the mouse. Administration of a single 200 mg/kg tamoxifen dose to pregnant wildtype C57BL/6J mice at gestational day 9.75 caused cleft palate and limb malformations in the fetuses, including posterior digit duplication, reduction, or fusion. These malformations were highly penetrant and consistent across independent chemical manufacturers. As opposed to 200 mg/kg, a single dose of 50 mg/kg tamoxifen at the same developmental stage did not result in overt structural malformations. Demonstrating that prenatal tamoxifen exposure at a specific time point causes dose-dependent developmental abnormalities, these findings argue for more considerate application of tamoxifen in Cre-inducible systems and further investigation of tamoxifen's mechanisms of action.

## Introduction

Tamoxifen is the oldest synthetic selective estrogen receptor (ER) modulator and is widely used in both clinical and basic research applications. Included in the World Health Organization list of essential medicines, tamoxifen is used to treat individuals with ER-positive breast cancer. Tamoxifen is also increasingly applied in biomedical research as part of powerful genetic recombination systems that leverage a fusion protein of Cre recombinase and a mutated ligand binding domain of the human ER (ERT). Upon tamoxifen binding to the ERT, nuclear translocation of the fusion protein facilitates Cre-mediated excision of loxP-flanked sequences in DNA [1]. Tamoxifen-inducible systems that allow temporally controlled genetic

study design, data collection and analysis, decision to publish, or preparation of the manuscript.

**Competing interests:** The authors have declared that no competing interests exist.

recombination are used for gene deletion, gene overexpression, and lineage tracing. This toolkit is applied to examine genetic, molecular, and cellular mechanisms, including those governing embryonic and postnatal development.

Although tamoxifen-inducible Cre models are widely employed to achieve temporal-specific gene alteration, developmental effects independent of Cre recombination have been suggested in multiple reports [2–10]. Animal model studies have shown that *in utero* tamoxifen exposure can cause mammary tumors, proliferative uterine lesions, oviduct hyperplasia, and impaired oocyte differentiation in offspring [5–7]. However, some reports also suggest that tamoxifen may have additional impacts on development that are not linked to ER signaling and endocrine disruption. Two recent reports described structural malformations in mouse embryos following maternal tamoxifen treatment [8, 11], while published human case reports document congenital anomalies associated with tamoxifen treatment during pregnancy, including craniofacial and limb defects [9, 10].

Here, we examined the impact of acute prenatal tamoxifen exposure on embryonic development in wildtype C57BL/6J mice. Our findings demonstrate that prenatal tamoxifen exposure causes structural limb and craniofacial malformations in a dose-dependent manner and suggest a previously unrecognized mechanism of action that may have significant implications for its use in clinical and basic research settings.

## Results

### Tamoxifen-induced malformations

Timed pregnant wildtype C57BL/6J mice were administered a single dose of 50 mg/kg or 200 mg/kg tamoxifen (Sigma) or vehicle alone by IP injection at gestational day (GD)9.75. Dams were euthanized at GD17, and uteri were carefully inspected. The number of live fetuses and resorptions in each litter as well as mean crown-rump length were calculated (Table 1). No statistically significant differences in average number of surviving fetuses, average number of resorptions, or average fetal crown-rump length were detected between treatment groups. No overt structural malformations were observed in either the vehicle-exposed control group (Fig 1A, 1A', 1F, 1F', 1I, 1I') or in the 50 mg/kg tamoxifen-exposed group. In the 200 mg/kg tamoxifen dose group, limb malformations were observed including posterior digit reduction (Fig 1B and 1C), posterior digit duplication with or without fusion (Fig 1D, 1G and 1H), and other distal limb defects (Fig 1E). Bone and cartilage staining of animals with gross limb malformations further revealed abnormalities in the metacarpals and phalanges (Fig 1B'–1E', 1G' and 1H'). Inspection of the oral cavity also revealed cleft palate in the group exposed to 200 mg/kg tamoxifen (Fig 1J and 1J') but not in the group exposed to 50 mg/kg tamoxifen.

The incidence of tamoxifen-induced structural malformations as visualized by whole mount brightfield imaging is shown in Fig 2. In the 200 mg/kg treatment group, gross structural malformations were observed in 59.14% of fetuses collected (n = 55/93) with affected fetuses identified in 15/21 litters. The majority of affected fetuses exhibited limb malformations (n = 54/93) including apparent posterior digit duplication with or without fusion (n = 48/54), apparent posterior digit reduction (n = 16/54), or other defects (n = 10/54). Limb abnormality patterns within individually affected fetuses were diverse and included both reduction and duplication phenotypes in separate limbs (n = 10/54), duplication and non-reduction/duplication phenotypes in separate limbs (n = 8/54), and reduction and non-reduction/duplication phenotype in separate limbs (n = 2/54). Malformations were present in both hindlimbs and forelimbs (n = 30/54), restricted to forelimbs (n = 11/54), or restricted to hindlimbs (n = 13/54). Cleft palate was observed in 20.43% of fetuses (n = 19/93), with 18 of 19 fetuses with cleft palate also exhibiting limb malformations.

**Table 1. Descriptors of the wildtype C57BL/6J study population found in Fig 2.**

Treatment (Distributor)	Litters Collected	Live Fetuses (Mean $\pm$ SD)	Resorptions (Mean $\pm$ SD)	Crown-rump Mean $\pm$ SD (mm)
Vehicle	9	52 (5.8 $\pm$ 1.91)	14 (1.56 $\pm$ 1.61)	16.63 $\pm$ 0.73
TAM 50 mg/kg (Sigma)	11	67 (6.1 $\pm$ 2.07)	13 (1.18 $\pm$ 1.40)	17.03 $\pm$ 1.24
TAM 200 mg/kg (Sigma)	21	93 (4.4 $\pm$ 2.85)	61 (2.90 $\pm$ 2.89)	16.80 $\pm$ 1.08
TAM 200 mg/kg (Selleckchem)	3	18 (6 $\pm$ 3.56)	1 (0.33 $\pm$ 0.47)	16.25 $\pm$ 1.12

Timed-pregnant wildtype C57BL/6J mice were administered the indicated doses of tamoxifen (TAM) at gestational day (GD)9.75 and inspected at GD17 for live fetuses and resorptions. One-way ANOVA was used to compare mean numbers of live fetuses, resorptions, and crown-rump lengths between vehicle- and TAM-treated groups. No statistically significant differences were detected across treatment groups. TAM, tamoxifen; SD, standard deviation.

<https://doi.org/10.1371/journal.pone.0256299.t001>

To test whether these outcomes were dependent upon chemical manufacturer, a parallel trial was conducted using tamoxifen supplied by an independent manufacturer and distributor (Selleckchem). No statistical differences in average number of surviving fetuses, average number of resorptions, or fetal crown-rump length were detected when comparing the 200 mg/kg Selleckchem tamoxifen group against the 200 mg/kg Sigma tamoxifen group and vehicle-exposed groups (Table 1). In the 200 mg/kg Selleckchem tamoxifen group, malformations were observed in 83.33% of fetuses ( $n = 15/18$ ), with affected individuals identified in each of the 3 litters. All affected fetuses exhibited limb malformations, including posterior digit duplication with or without fusion ( $n = 15/15$ ), posterior digit reduction ( $n = 5/15$ ), or other defects ( $n = 3/15$ ). All animals that exhibited a posterior digit reduction or other defect additionally exhibited a duplication malformation. In this tamoxifen (Selleckchem) cohort, most affected fetuses exhibited malformations affecting both the fore- and hindlimbs ( $n = 12/15$ ), while a minority had only forelimb ( $n = 1/15$ ) or only hindlimb abnormalities ( $n = 2/15$ ). Cleft palate was 16.67% penetrant in these fetuses ( $n = 3/18$ ) and always accompanied by limb malformations.

## Discussion

The tamoxifen/CreERT genetic recombination system is a powerful and widely used approach to examine molecular and cellular mechanisms of development and disease. However, off-target effects of tamoxifen treatment, including Cre toxicity [12], may confound interpretation of results from the use of these models [13]. Previous studies examining the potential of tamoxifen to affect developmental processes have focused upon outcomes related to endocrine modulation. Here, we demonstrate that *in utero* high-dose tamoxifen exposure results in developmental abnormalities in the absence of genetic recombination and causing structural malformations in wildtype C57BL/6J mice. Specifically, we found that prenatal tamoxifen exposure at a precise critical period of development results in malformations of the limbs and palate. These findings are consistent with several published reports of prenatal tamoxifen exposure. One clinical case report described limb (“club foot”) and craniofacial (micrognathia and cleft palate) malformations in a child exposed to tamoxifen during the first trimester [14]. Two recent reports noted structural malformations in mice exposed to tamoxifen *in utero*, including neural tube defects, cleft palate, and eye abnormalities [8, 11]. These observations suggest that tamoxifen has off-target effects that may impact its use in mouse model research and that usage of lower doses may be a strategy to mitigate these off-target effects.

Tamoxifen is used in CreERT transgenic models to trigger temporally specific Cre-recombinase activity in adult mice, neonates, and embryos and fetuses *in utero* via maternal administration. Across published studies, protocols for tamoxifen administration to pregnant dams in order to induce recombination in embryos vary considerably with respect to preparation, route, dose, duration of exposure, and co-administration with other drugs such as

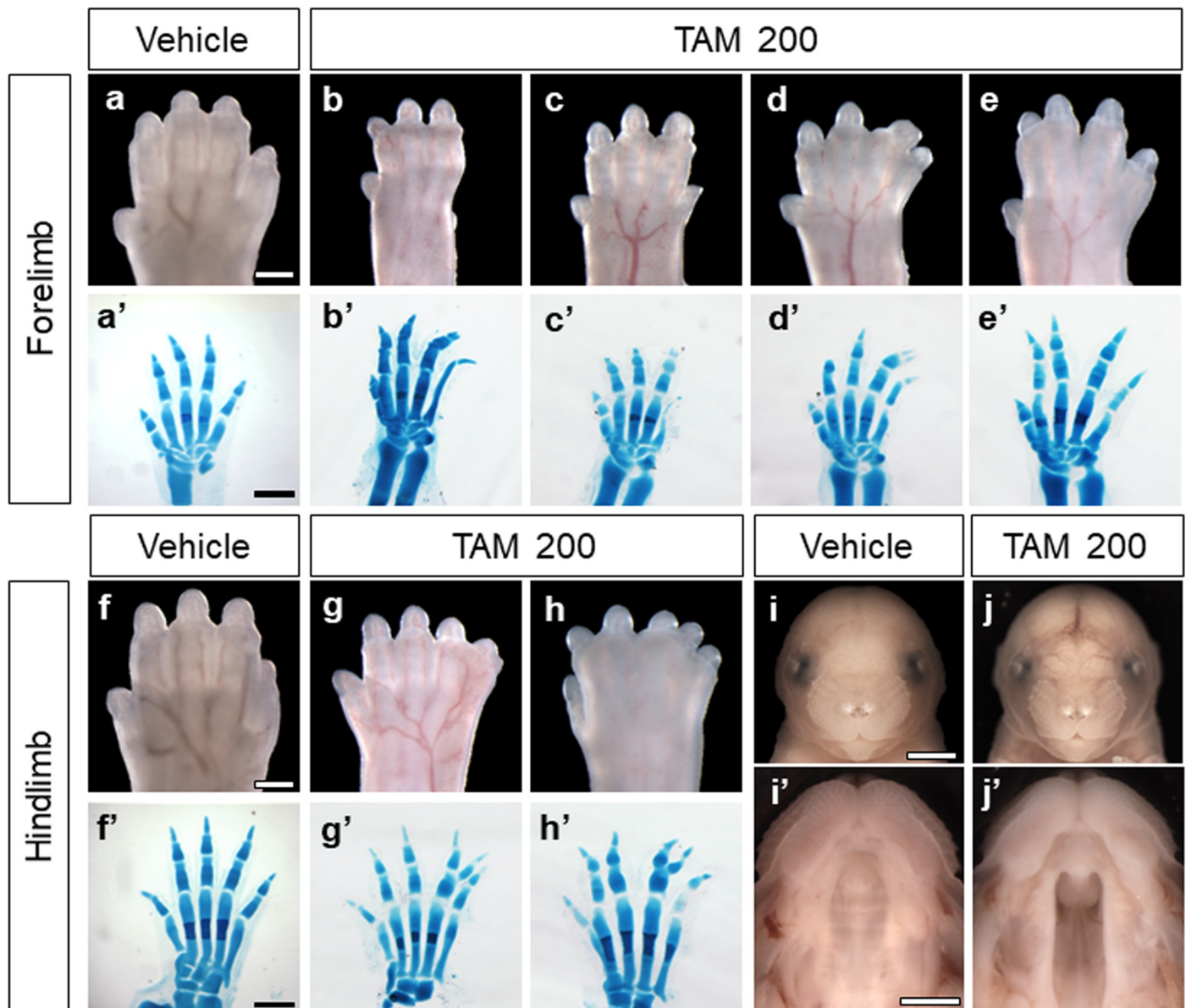


**Fig 1. Tamoxifen-induced limb and craniofacial malformations.** Along with representative vehicle controls of forelimb (a), hindlimb (f), and palate (i'), examples of malformations in forelimbs (b-e), hindlimbs (g, h), and palate (j') of 200 mg/kg tamoxifen-treated animals are shown at GD17. Bone and cartilage staining of tamoxifen-treated animals revealed underlying skeletal abnormalities compared to controls (a'-h'). In the forelimbs of animals with reduction malformations (b, c), dysmorphism in both the metacarpals and phalanges of the 5<sup>th</sup> digit are apparent. Additionally, the distal-most phalanx of the 4<sup>th</sup> digit appears to be duplicated in these animals (b', c'). An animal with a forelimb duplication malformation (d) exhibited a replication of the distal phalanx of the 4<sup>th</sup> digit (d'). In hindlimbs of animals with duplication malformations (g, h), staining revealed replications of the distal and middle phalanges of the 4<sup>th</sup> digit (g', h'). In an animal with a non-reduction/duplication phenotype (e), no overt skeletal abnormalities are apparent (e'). Secondary cleft palate (j') was also observed in 200 mg/kg tamoxifen-treated animals. TAM, tamoxifen. Scale bars in a, a', f, and f': 0.5 mm; Scale bar in i: 2.0 mm; Scale bar in i': 1.0 mm.

<https://doi.org/10.1371/journal.pone.0256299.g001>

progesterone [15–39]. In this study, we chose a single IP administration of 50 or 200 mg/kg to encompass commonly utilized administration regimens [19, 26, 36–39]. We also tested whether developmental effects caused by tamoxifen were consistent across multiple suppliers of tamoxifen. While a high dose of tamoxifen from both suppliers caused structural malformations, there was a (not statistically significant) trend toward higher resorptions and lower malformation penetrance in the Sigma cohort and lower resorptions and higher malformation

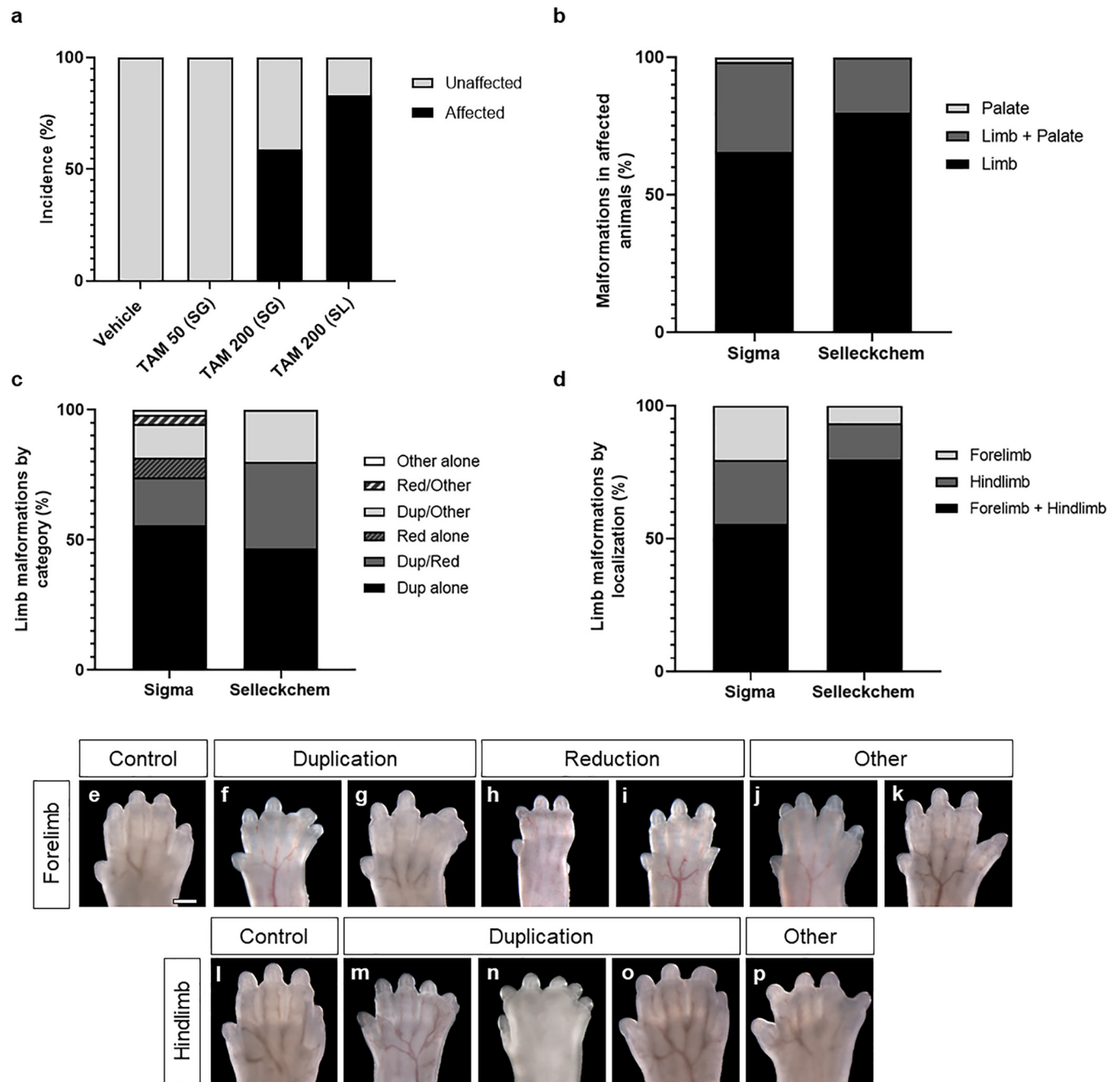


**Fig 2. Incidence of tamoxifen-induced limb and craniofacial malformations.** The incidence of malformations occurring in animals treated with tamoxifen or vehicle at GD9.75 are summarized (a-d). The percentage of animals displaying at least one structural malformation in each treatment group is shown (a). Structural malformations appeared in animals treated with 200 mg/kg Sigma or Selleckchem tamoxifen, and these affected animals displayed either limb malformations, craniofacial malformations, or co-occurring limb and craniofacial malformations (b). Except for a single animal exhibiting an isolated secondary cleft palate, all affected animals exhibited limb malformations (b). Therefore, limb abnormalities were further classified according to apparent dysmorphology (c) and limb-specific localization of the abnormality (d). Examples of limb morphology in vehicle controls and tamoxifen-treated animals (e-p). A duplication phenotype was assigned to limbs that exhibited an extra posterior digit with or without cutaneous fusion to adjacent digits in both forelimbs (f, g) and hindlimbs (m, n, o). Posterior digit reduction phenotypes were exclusive to forelimbs and included apparent absence of a 5<sup>th</sup> digit (h), or a shortening of the 5<sup>th</sup> digit (i). Non-reduction/duplication phenotypes included apparent hyperplasia of interdigital tissue between the 2<sup>nd</sup> and 3<sup>rd</sup> forelimb digits (j) and laterally displaced 5<sup>th</sup> digits in forelimbs (k) and hindlimbs (p). Scale bar in a: 0.5 mm. TAM, tamoxifen; SG, Sigma; SL, Selleckchem; Dup, duplication; Red, reduction.

<https://doi.org/10.1371/journal.pone.0256299.g002>

penetrance in the Selleckchem cohort. Whether the activity demonstrated here for tamoxifen administration is retained by other tamoxifen manufacturers, administration routes, drug preparations, or administration of tamoxifen metabolites that also activate ERT (*e.g.*, 4-hydroxytamoxifen) is unclear and should be examined.

The observations reported herein follow two recent reports of structural malformations in wildtype mice following prenatal tamoxifen exposure. In one report, repeated tamoxifen exposure targeting slightly later critical periods of development (~GD10.5–13.5) was found to cause cleft palate [11]. In another report, embryos and fetuses from pregnant dams dosed with 10–200 mg/kg tamoxifen between GD5.5 and GD7.5 exhibited abnormal development and malformations, including neural tube defects, cleft palate, and eye abnormalities [8]. In this previous study, 8 out of 8 dams were reported to develop severe intrauterine hemorrhaging, and maternal toxicity was implicated as a causal or contributing factor to the observed developmental outcomes. The observations collected for the study described herein, however, are not consistent with a significant role for maternal toxicity in causing the malformations that followed targeted administration of tamoxifen. In our study cohort of wildtype C57BL/6J mice, a total of 11 dams were treated with 50 mg/kg tamoxifen and 24 dams were treated with 200 mg/kg tamoxifen at GD9.75. Signs of overt maternal toxicity were not observed, and no significant differences were detected in litter size at GD17, number of resorbs, or crown-rump lengths of fetuses (Table 1). Rather than a constellation of developmental outcomes, targeted tamoxifen exposure produced consistent and specific malformations that, to our knowledge, are not associated with maternal toxicity. While a role of maternal toxicity cannot be excluded, the observations reported herein better align with the premise that tamoxifen disrupts embryonic developmental through a currently unknown mechanism.

Tamoxifen's biological effects are thought to be predominantly mediated through its binding to ER $\alpha$  and ER $\beta$  [40, 41]. To our knowledge, neither limb nor palate malformations have been reported to directly result from endocrine disruption and have not been reported in *Esr1* (ER $\alpha$ ) or *Esr2* (ER $\beta$ ) knockout mice [42, 43]. We performed preliminary experiments to examine the impact of *in utero* tamoxifen exposure in *Esr1*<sup>-/-</sup> and *Esr2*<sup>-/-</sup> mice (Jax strains 026176 and 004745, respectively) where timed-pregnant dams were administered 200 mg/kg tamoxifen (Sigma) at GD9.75, and structural malformations in offspring were examined at GD17 as in our wildtype cohort. While the sample size generated was not large enough for statistical analyses of malformation incidence across each genotype, limb malformations were observed in some *Esr1*<sup>-/-</sup> and *Esr2*<sup>-/-</sup> fetuses (S1 Fig and S1 and S2 Tables). A previous study also reported that mRNA expression of *Esr1* and *Esr2* was not detected in the limb during the critical period examined here for tamoxifen-induced limb malformations [44]. Together, these findings suggest that the mechanism by which tamoxifen exposure results in structural malformations may be independent of ER signaling, but determining whether ER or G protein coupled ER signaling plays any role in tamoxifen-induced structural malformations will require further investigation.

While thought to act predominantly through ER signaling, tamoxifen has previously been shown to affect processes such as proliferation, apoptosis, and angiogenesis through ER-independent mechanisms [45–54]. Additionally, tamoxifen or its metabolites have been reported to directly bind to off-target receptors such as aryl hydrocarbon receptor [55] and histamine, muscarinic, and dopamine receptors [53]. Previous studies have also reported that tamoxifen potently interferes with cholesterol synthesis *in vitro* and *in vivo* and that this activity is ER-independent [56–58]. Several signaling pathways are dependent upon cholesterol biosynthesis, including the Sonic hedgehog (Shh) signaling pathway. Covalent binding of cholesterol produces fully active SHH peptide that initiates signaling in effector cells through the Smoothed protein [59], the activity of which was recently also shown to be dependent upon cholesterol binding [60, 61]. Shh signaling plays multiple roles in development including craniofacial and

limb morphogenesis, and disruption of this pathway at the same time point as the one used in this study has been shown to cause cleft palate and limb malformations [62], consistent with those reported herein to result from *in utero* tamoxifen exposure. This period during development encompasses major tissue patterning events, including limb and orofacial morphogenesis, and these processes may be particularly susceptible to chemical perturbation [63]. Future investigation into the mechanism(s) underlying the biological impacts of tamoxifen should benefit from demonstration herein that *in utero* tamoxifen exposure at a specific critical period in development results in specific malformations.

Here, we present a previously unreported action of tamoxifen that may have important implications for its use in both clinical and basic research settings. Demonstrating that a high dose of tamoxifen during a specific critical period in development causes structural malformations in the absence of genetic recombination suggests previously undescribed mechanisms for this widely used drug. We focused on structural malformations because they are novel, robust, and highly penetrant, but the importance of understanding whether and how tamoxifen acts through additional mechanisms is likely not limited to developmental contexts, as most developmental signaling pathways play roles in postnatal homeostasis, healing and repair, and disease processes. These findings, along with other reports illustrating off-target effects in utilization of CreERT models, support a more considerate use of these systems and interpretation of generated experimental results.

## Methods

### Materials

Tamoxifen used in these studies was obtained from two independent chemical distributors. Tamoxifen from MilliporeSigma (Catalog No. T5648, Lot No. WXBC7537V) was manufactured by AstraZeneca and had a supplier-stated purity of 99.00%. In this study, tamoxifen from MilliporeSigma is abbreviated as “Sigma”. Tamoxifen from Selleckchem (Catalog No. S1238, Lot No. S123802) was manufactured by Selleckchem and had a supplier-stated purity of 99.04%. Both vendors reported tamoxifen to have a solubility of 50 mg/ml in DMSO as well as a melting point between 96–98°C.

### Timed mouse mating

These studies were conducted in strict accordance with the recommendations in the *Guide for the Care and Use of Laboratory Animals* of the National Institute of Health. The protocol was approved by the University of Wisconsin School of Veterinary Medicine Institutional Animal Care and Use Committee (Protocol No. 13–081.0). Wildtype C57BL/6J (Strain No. 00664) mice were purchased from The Jackson Laboratory and housed under specific pathogen-free conditions in disposable, ventilated cages. Rooms were maintained at  $22 \pm 2^\circ\text{C}$  and 30–70% humidity on a 12-h light, 12-h dark cycle. Mice were fed Irradiated Soy Protein-Free Extruded Rodent Diet (Catalog No. 2920x; Envigo Teklad Global) until day of plug, when dams received Irradiated Teklad Global 19% Protein Extruded Rodent Diet (Catalog No. 2919; Envigo Teklad Global). For timed matings, 1–2 nulliparous female mice were placed with a single male for 1–2 h and subsequently examined for the presence of copulation plugs as previously described [64]. The beginning of the mating period was designated as gestational day (GD)0.

### Tamoxifen exposure

Tamoxifen (Sigma or Selleckchem) was dissolved into solution with corn oil (Acros Organics). Aliquots were stored at 4°C and used within 3 weeks of preparation. Pregnant mice were

administered an intraperitoneal (IP) injection of either 50 mg/kg tamoxifen, 200 mg/kg tamoxifen, or corn oil vehicle at GD9.75 ± 0.05.

### Dissection and imaging

Pregnant females were euthanized by CO<sub>2</sub> asphyxiation followed by cervical dislocation at GD17 ± 2 h. Fetuses were placed in phosphate buffered saline on ice for no less than 30 min before dissection. Crown-rump measurements and initial gross phenotyping were conducted before fetal specimens were fixed in 10% formalin for at least 24 h before imaging. Images were taken of whole body, face, and palate using a MicroPublisher 5.0 camera connected to an Olympus SZX-10 stereomicroscope.

### Phenotypic assessment

Fetuses were assessed for gross malformations by thorough visual inspection. For each fetus, whole mount brightfield images were captured to document morphology, with a focus on the limbs and craniofacial regions. Limb malformations were grouped into one of three classes of overt distal limb abnormalities: apparent posterior digit duplication with or without fusion, apparent posterior digit reduction, and additional defects that do not exhibit overt digit reduction or duplication (Fig 2E–2P). Craniofacial malformations were characterized by the presence of secondary palate clefting. Animals were classified as affected by displaying at least one of these malformations.

### Bone & cartilage staining

Bone and cartilage staining was employed to reveal underlying skeletal abnormalities in animals classified as affected based upon careful scrutiny of light images. Following euthanasia, fetal specimens with overt structural malformations were skinned, eviscerated, and fixed in 95% or 100% ethanol for at least 3 d, then placed overnight in an alcian blue staining solution containing 8 ml of 100% ethanol, 10 ml of 100% glacial acetic acid, and 2 ml of 1% alcian blue in 3% acetic acid. They were then rinsed twice for 1 h and subsequently left overnight in 100% ethanol. Following clearing for 2 h in 1% potassium hydroxide, staining in 0.005% alizarin red in 2% potassium hydroxide for 4 h was performed. Fetuses were then rinsed in 2% potassium hydroxide once quickly, once for 1 h, and then left overnight in 1% potassium hydroxide. Finally, they were transferred to 1:3 solution of glycerol: 2% potassium hydroxide for 8 h and stored and imaged in a 1:1 solution of glycerol: 2% potassium hydroxide.

### Statistics

Graphpad Prism 8 was used for all statistical analyses. One-way analysis of variance (ANOVA) with Tukey's post hoc test for multiple comparisons was used for analyses of litter sizes, resorptions, and crown-rump lengths. An alpha value of 0.05 was maintained for determination of significance for all experiments.

### Supporting information

**S1 Fig. Structural malformations in *Esr1* and *Esr2* animals.** Representative examples of distal limb dysmorphology in hindlimbs of 200 mg/kg tamoxifen-treated animals (b, d, f, h) are shown along with vehicle controls (a, c, e, g). TAM 200, tamoxifen 200 mg/kg. Scale bars in a, e: 0.5 mm.

(TIF)



**S1 Table. Descriptors of the *Esr1* and *Esr2* study populations.** Female *Esr1*<sup>+/-</sup> mice were mated with male *Esr1*<sup>+/-</sup> mice, and female *Esr2*<sup>+/-</sup> mice were mated with either *Esr2*<sup>+/-</sup> or *Esr2*<sup>-/-</sup> male mice. Timed-pregnant dams were administered 200 mg/kg of tamoxifen at gestational day (GD)9.75. At GD17, dams were inspected for live fetuses and resorptions, and fetuses were measured for crown-rump length and genotyped from tail tissue. TAM, tamoxifen; SD, standard deviation.

(DOCX)

**S2 Table. Incidence of malformations by genotype in *Esr1* and *Esr2* animals.** Incidence of limb malformations, cleft palate, or limb malformations or cleft palate are listed for each genotype and treatment group of the *Esr1* and *Esr2* study populations. TAM, tamoxifen.

(DOCX)

## Acknowledgments

The authors are grateful to Eric Sandgren and Linda Schuler for critical discussion, Kristen Uchtmann and William Ricke for sharing reagents, and the University of Wisconsin-Madison Biotron Laboratory and the University of Wisconsin Biomedical Research Model Services Mouse Breeding Core for providing research services.

## Author Contributions

**Conceptualization:** Miranda R. Sun, Robert J. Lipinski.

**Formal analysis:** Austin C. Steward, Emma A. Sweet.

**Funding acquisition:** Robert J. Lipinski.

**Investigation:** Miranda R. Sun, Austin C. Steward, Emma A. Sweet, Alexander A. Martin.

**Methodology:** Miranda R. Sun, Austin C. Steward, Emma A. Sweet.

**Project administration:** Robert J. Lipinski.

**Supervision:** Robert J. Lipinski.

**Visualization:** Austin C. Steward, Emma A. Sweet.

**Writing – original draft:** Miranda R. Sun, Austin C. Steward, Emma A. Sweet, Robert J. Lipinski.

**Writing – review & editing:** Alexander A. Martin.

## References

1. Metzger D, Chambon P. Site- and time-specific gene targeting in the mouse. *Methods*. 2001; 24(1):71–80. <https://doi.org/10.1006/meth.2001.1159> PMID: 11327805.
2. GC C, GA B, LA L, PJ S, WL M. Abnormal Reproductive Development in Rats After Neonatally Administered Antiestrogen (Tamoxifen). *Biology of reproduction*. 1979; 21(5). <https://doi.org/10.1095/biolreprod21.5.1087> PMID: 574777.
3. T I, M H, N T. Occurrence of Genital Tract Abnormalities and Bladder Hernia in Female Mice Exposed Neonatally to Tamoxifen. *Toxicology*. 1986; 42(1). [https://doi.org/10.1016/0300-483x\(86\)90087-9](https://doi.org/10.1016/0300-483x(86)90087-9) PMID: 3798455.
4. GR C, O T, R N, Y N, SJ R. Teratogenic Effects of Clomiphene, Tamoxifen, and Diethylstilbestrol on the Developing Human Female Genital Tract. *Human pathology*. 1987; 18(11). [https://doi.org/10.1016/s0046-8177\(87\)80381-7](https://doi.org/10.1016/s0046-8177(87)80381-7) PMID: 3679188.
5. L H-C, E C, I O, DJ L, R C. Maternal Exposure to Tamoxifen During Pregnancy Increases Carcinogen-Induced Mammary Tumorigenesis Among Female Rat Offspring. *Clinical cancer research: an official journal of the American Association for Cancer Research*. 2000; 6(1). PMID: 10656462.

6. L R, JS R, K A. Maternal Tamoxifen Treatment Alters Oocyte Differentiation in the Neonatal Mice: Inhibition of Oocyte Development and Decreased Folliculogenesis. *The journal of obstetrics and gynaecology research*. 2010; 36(2). <https://doi.org/10.1111/j.1447-0756.2009.01129.x> PMID: 20492370.
7. BA D, LM A, JM W. Proliferative Lesions of Oviduct and Uterus in CD-1 Mice Exposed Prenatally to Tamoxifen. *Carcinogenesis*. 1997; 18(10). <https://doi.org/10.1093/carcin/18.10.2009> PMID: 9364013.
8. Ved N, Curran A, Ashcroft FM, Sparrow DB. Tamoxifen administration in pregnant mice can be deleterious to both mother and embryo. <https://doi.org/10.1177/0023677219856918>.
9. Braems G, Denys H, De Wever O, Cocquyt V, Van den Broecke R. Use of Tamoxifen Before and During Pregnancy. *Oncologist*. 162011. p. 1547–51.
10. Tewari K, Perinatology Division DoOaG, Women's Hospital, Memorial Medical Center, Long Beach, California, and Division of Pediatric Urology and Urologic Oncology DoU, University of California, Bonebrake RG, Perinatology Division DoOaG, Women's Hospital, Memorial Medical Center, Long Beach, California, and Division of Pediatric Urology and Urologic Oncology DoU, University of California, et al. Ambiguous genitalia in infant exposed to tamoxifen in utero. Elsevier, 1997 1997/07/19. Report No.: 1474-547X Contract No.: 9072.
11. Xu J, Huang Z, Wang L, Li H, Zhang Y, Shao M, et al. Tamoxifen exposure induces cleft palate in mice. *Br J Oral Maxillofac Surg*. 2021; 59(1):52–7. Epub 2020/07/25. <https://doi.org/10.1016/j.bjoms.2020.07.009> PMID: 32723574.
12. Brash JT, Bolton RL, Rashbrook VS, Denti L, Kubota Y, Ruhrberg C. Tamoxifen-Activated CreERT Impairs Retinal Angiogenesis Independently of Gene Deletion. *Circ Res*. 2020; 127(6):849–50. Epub 2020/07/08. <https://doi.org/10.1161/CIRCRESAHA.120.317025> PMID: 32635822; PubMed Central PMCID: PMC7447161.
13. Wüst RCI, Houtkooper RH, Auwerx J. Confounding factors from inducible systems for spatiotemporal gene expression regulation. *J Cell Biol*. 2020; 219(7). <https://doi.org/10.1083/jcb.202003031> PMID: 32428200; PubMed Central PMCID: PMC7337492.
14. Berger JC, Clericuzio CL. Pierre Robin sequence associated with first trimester fetal tamoxifen exposure. *Am J Med Genet A*. 2008; 146A(16):2141–4. <https://doi.org/10.1002/ajmg.a.32432> PMID: 18629878.
15. PS D, D M, DH R, SK M, AP M. Modification of Gene Activity in Mouse Embryos in Utero by a Tamoxifen-Inducible Form of Cre Recombinase. *Current biology: CB*. 1998; 8(24). [https://doi.org/10.1016/S0960-9822\(07\)00562-3](https://doi.org/10.1016/S0960-9822(07)00562-3) PMID: 9843687.
16. Jin H, Wang H, Li J, Yu S, Xu M, Qiu Z, et al. Differential contribution of the two waves of cardiac progenitors and their derivatives to aorta and pulmonary artery. *Dev Biol*. 2019; 450(2):82–9. Epub 2019/04/02. <https://doi.org/10.1016/j.ydbio.2019.03.019> PMID: 30951706.
17. Ellis D, Zervas M. Tamoxifen dose response and conditional cell marking: is there control? *Mol Cell Neurosci*. 2010; 45(2):132–8. Epub 2010/06/17. <https://doi.org/10.1016/j.mcn.2010.06.004> PMID: 20600933.
18. Weber T, Böhm G, Hermann E, Schütz G, Schöning K, Bartsch D. Inducible gene manipulations in serotonergic neurons. *Front Mol Neurosci*. 2009; 2:24. Epub 2009/11/06. <https://doi.org/10.3389/neuro.02.024.2009> PMID: 19936315; PubMed Central PMCID: PMC2779094.
19. Bonnamour G, Soret R, Pilon N. Dhh-expressing Schwann cell precursors contribute to skin and cochlear melanocytes, but not to vestibular melanocytes. *Pigment Cell Melanoma Res*. 2021; 34(3):648–54. Epub 2020/11/03. <https://doi.org/10.1111/pcmr.12938> PMID: 33089656.
20. El Agha E, Al Alam D, Carraro G, MacKenzie B, Goth K, De Langhe SP, et al. Characterization of a novel fibroblast growth factor 10 (Fgf10) knock-in mouse line to target mesenchymal progenitors during embryonic development. *PLoS One*. 2012; 7(6):e38452. Epub 2012/06/13. <https://doi.org/10.1371/journal.pone.0038452> PMID: 22719891; PubMed Central PMCID: PMC3374781.
21. Savery D, Maniou E, Culshaw LH, Greene NDE, Copp AJ, Galea GL. Refinement of inducible gene deletion in embryos of pregnant mice. *Birth Defects Res*. 2020; 112(2):196–204. Epub 2019/12/03. <https://doi.org/10.1002/bdr2.1628> PMID: 31793758; PubMed Central PMCID: PMC7003956.
22. Tang Q, Xu M, Xu J, Xie X, Yang H, Gan L. Gfi1-GCE inducible Cre line for hair cell-specific gene manipulation in mouse inner ear. *Genesis*. 2019; 57(9):e23304. Epub 2019/05/11. <https://doi.org/10.1002/dvg.23304> PMID: 31077553.
23. Schneider S, Hotaling N, Campos M, Patnaik SR, Bharti K, May-Simera HL. Generation of an inducible RPE-specific Cre transgenic-mouse line. *PLoS One*. 2018; 13(11):e0207222. Epub 2018/11/15. <https://doi.org/10.1371/journal.pone.0207222> PMID: 30440011; PubMed Central PMCID: PMC6237357.
24. Huang W, Guo Q, Bai X, Scheller A, Kirchoff F. Early embryonic NG2 glia are exclusively gliogenic and do not generate neurons in the brain. *Glia*. 2019; 67(6):1094–103. Epub 2019/02/06. <https://doi.org/10.1002/glia.23590> PMID: 30724411.

25. Huang W, Bai X, Stopper L, Catalin B, Cartarozzi LP, Scheller A, et al. During Development NG2 Glial Cells of the Spinal Cord are Restricted to the Oligodendrocyte Lineage, but Generate Astrocytes upon Acute Injury. *Neuroscience*. 2018; 385:154–65. Epub 2018/06/18. <https://doi.org/10.1016/j.neuroscience.2018.06.015> PMID: 29913244.
26. Gil-Sanz C, Espinosa A, Fregoso SP, Bluske KK, Cunningham CL, Martinez-Garay I, et al. Lineage Tracing Using Cux2-Cre and Cux2-CreERT2 Mice. *Neuron*. 2015; 86(4):1091–9. <https://doi.org/10.1016/j.neuron.2015.04.019> PMID: 25996136; PubMed Central PMCID: PMC4455040.
27. Hagan AS, Boylan M, Smith C, Perez-Santamarina E, Kowalska K, Hung IH, et al. Generation and validation of novel conditional flox and inducible Cre alleles targeting fibroblast growth factor 18 (Fgf18). *Dev Dyn*. 2019; 248(9):882–93. Epub 2019/07/22. <https://doi.org/10.1002/dvdy.85> PMID: 31290205; PubMed Central PMCID: PMC7029619.
28. Takenoshita M, Takechi M, Vu Hoang T, Furutera T, Akagawa C, Namangkalakul W, et al. Cell lineage and expression-based inference of the roles of forkhead box transcription factor Foxc2 in craniofacial development. *Dev Dyn*. 2021. Epub 2021/03/05. <https://doi.org/10.1002/dvdy.324> PMID: 33667029.
29. Holl AM. Survival of mature mouse olfactory sensory neurons labeled genetically perinatally. *Mol Cell Neurosci*. 2018; 88:258–69. Epub 2018/02/07. <https://doi.org/10.1016/j.mcn.2018.02.005> PMID: 29427775.
30. Tsai YH, Hill DR, Kumar N, Huang S, Chin AM, Dye BR, et al. LGR4 and LGR5 Function Redundantly During Human Endoderm Differentiation. *Cell Mol Gastroenterol Hepatol*. 2016; 2(5):648–62.e8. Epub 2016/06/23. <https://doi.org/10.1016/j.jcmgh.2016.06.002> PMID: 28078320; PubMed Central PMCID: PMC5042889.
31. Ackermann AM, Zhang J, Heller A, Briker A, Kaestner KH. High-fidelity Glucagon-CreER mouse line generated by CRISPR-Cas9 assisted gene targeting. *Mol Metab*. 2017; 6(3):236–44. Epub 2017/01/12. <https://doi.org/10.1016/j.molmet.2017.01.003> PMID: 28271030; PubMed Central PMCID: PMC5323890.
32. Chrysostomou E, Zhou L, Darcy YL, Graves KA, Doetzlhofer A, Cox BC. The Notch Ligand Jagged1 Is Required for the Formation, Maintenance, and Survival of Hensen's Cells in the Mouse Cochlea. *J Neurosci*. 2020; 40(49):9401–13. Epub 2020/10/30. <https://doi.org/10.1523/JNEUROSCI.1192-20.2020> PMID: 33127852; PubMed Central PMCID: PMC7724135.
33. Deal KK, Rosebrock JC, Eeds AM, DeKeyser JL, Musser MA, Ireland SJ, et al. Sox10-cre BAC transgenes reveal temporal restriction of mesenchymal cranial neural crest and identify glandular Sox10 expression. *Dev Biol*. 2021; 471:119–37. Epub 2020/12/13. <https://doi.org/10.1016/j.ydbio.2020.12.006> PMID: 33316258; PubMed Central PMCID: PMC7855809.
34. Martinez-Corral I, Stanczuk L, Frye M, Ulvmar MH, Diéguez-Hurtado R, Olmeda D, et al. Vegfr3-CreER (T2) mouse, a new genetic tool for targeting the lymphatic system. *Angiogenesis*. 2016; 19(3):433–45. Epub 2016/03/18. <https://doi.org/10.1007/s10456-016-9505-x> PMID: 26993803.
35. Lüdtke TH, Rudat C, Kurz J, Häfner R, Greulich F, Wojahn I, et al. Mesothelial mobilization in the developing lung and heart differs in timing, quantity, and pathway dependency. *Am J Physiol Lung Cell Mol Physiol*. 2019; 316(5):L767–L83. Epub 2019/01/31. <https://doi.org/10.1152/ajplung.00212.2018> PMID: 30702346.
36. El Shahawy M, Reibring CG, Neben CL, Hallberg K, Marangoni P, Harfe BD, et al. Cell fate specification in the lingual epithelium is controlled by antagonistic activities of Sonic hedgehog and retinoic acid. *PLoS Genet*. 2017; 13(7):e1006914. Epub 2017/07/17. <https://doi.org/10.1371/journal.pgen.1006914> PMID: 28715412; PubMed Central PMCID: PMC5536368.
37. Rockwell DM, O'Connor AK, Bentley-Ford MR, Haycraft CJ, Croyle MJ, Brewer KM, et al. A transgenic Alx4-CreER mouse to analyze anterior limb and nephric duct development. *Dev Dyn*. 2021. Epub 2021/03/16. <https://doi.org/10.1002/dvdy.328> PMID: 33728725.
38. Nakamura E, Nguyen MT, Mackem S. Kinetics of tamoxifen-regulated Cre activity in mice using a cartilage-specific CreER(T) to assay temporal activity windows along the proximodistal limb skeleton. *Dev Dyn*. 2006; 235(9):2603–12. <https://doi.org/10.1002/dvdy.20892> PMID: 16894608.
39. Lizen B, Claus M, Jeannotte L, Rijli FM, Gofflot F. Perinatal induction of Cre recombination with tamoxifen. *Transgenic Res*. 2015; 24(6):1065–77. Epub 2015/09/22. <https://doi.org/10.1007/s11248-015-9905-5> PMID: 26395370.
40. An KC. Selective Estrogen Receptor Modulators. *Asian Spine J*. 2016; 10(4):787–91. <https://doi.org/10.4184/asj.2016.10.4.787> PMID: 27559463; PubMed Central PMCID: PMC4995266.
41. M D, CL S. Molecular Mechanisms of Selective Estrogen Receptor Modulator (SERM) Action. *The Journal of pharmacology and experimental therapeutics*. 2000; 295(2). PMID: 11046073.
42. Lee HR, Kim TH, Choi KC. Functions and physiological roles of two types of estrogen receptors, ER $\alpha$  and ER $\beta$ , identified by estrogen receptor knockout mouse. *Lab Anim Res*. 2012; 28(2):71–6. <https://doi.org/10.5625/lar.2012.28.2.71> PMID: 22787479; PubMed Central PMCID: PMC3389841.

43. JF C, KS K. Estrogen Receptor Null Mice: What Have We Learned and Where Will They Lead Us? *Endocrine reviews*. 1999; 20(3). <https://doi.org/10.1210/edrv.20.3.0370> PMID: 10368776.
44. Lemmen JG, Broekhof JL, Kuiper GG, Gustafsson JA, van der Saag PT, van der Burg B. Expression of estrogen receptor alpha and beta during mouse embryogenesis. *Mech Dev*. 1999; 81(1–2):163–7. [https://doi.org/10.1016/s0925-4773\(98\)00223-8](https://doi.org/10.1016/s0925-4773(98)00223-8) PMID: 10330493.
45. Todorova VK, Kaufmann Y, Luo S, Klimberg VS. Tamoxifen and raloxifene suppress the proliferation of estrogen receptor-negative cells through inhibition of glutamine uptake. *Cancer Chemother Pharmacol*. 2011; 67(2):285–91. Epub 2010/04/11. <https://doi.org/10.1007/s00280-010-1316-y> PMID: 20383709.
46. Hasegawa G, Akatsuka K, Nakashima Y, Yokoe Y, Higo N, Shimonaka M. Tamoxifen inhibits the proliferation of non-melanoma skin cancer cells by increasing intracellular calcium concentration. *Int J Oncol*. 2018; 53(5):2157–66. Epub 2018/08/31. <https://doi.org/10.3892/ijo.2018.4548> PMID: 30226592.
47. Benson JR, Wakefield LM, Baum M, Colletta AA. Synthesis and secretion of transforming growth factor beta isoforms by primary cultures of human breast tumour fibroblasts in vitro and their modulation by tamoxifen. *Br J Cancer*. 1996; 74(3):352–8. <https://doi.org/10.1038/bjc.1996.365> PMID: 8695348; PubMed Central PMCID: PMC2074642.
48. Ferlini C, Scambia G, Marone M, Distefano M, Gaggini C, Ferrandina G, et al. Tamoxifen induces oxidative stress and apoptosis in oestrogen receptor-negative human cancer cell lines. *Br J Cancer*. 1999; 79(2):257–63. <https://doi.org/10.1038/sj.bjc.6690042> PMID: 9888466; PubMed Central PMCID: PMC2362195.
49. Huh WJ, Khurana SS, Geahlen JH, Kohli K, Waller RA, Mills JC. Tamoxifen induces rapid, reversible atrophy, and metaplasia in mouse stomach. *Gastroenterology*. 2012; 142(1):21-4.e7. Epub 2011/10/14. <https://doi.org/10.1053/j.gastro.2011.09.050> PMID: 22001866; PubMed Central PMCID: PMC3708546.
50. Johnson KE, Forward JA, Tippy MD, Ceglowski JR, El-Husayni S, Kulenthirarajan R, et al. Tamoxifen Directly Inhibits Platelet Angiogenic Potential and Platelet-Mediated Metastasis. *Arterioscler Thromb Vasc Biol*. 2017; 37(4):664–74. Epub 2017/02/02. <https://doi.org/10.1161/ATVBAHA.116.308791> PMID: 28153880; PubMed Central PMCID: PMC5364056.
51. Blackwell KL, Haroon ZA, Shan S, Saito W, Broadwater G, Greenberg CS, et al. Tamoxifen inhibits angiogenesis in estrogen receptor-negative animal models. *Clin Cancer Res*. 2000; 6(11):4359–64. PMID: 11106254.
52. Shim JS, Li RJ, Lv J, Head SA, Yang EJ, Liu JO. Inhibition of angiogenesis by selective estrogen receptor modulators through blockade of cholesterol trafficking rather than estrogen receptor antagonism. *Cancer Lett*. 2015; 362(1):106–15. Epub 2015/03/20. <https://doi.org/10.1016/j.canlet.2015.03.022> PMID: 25799952; PubMed Central PMCID: PMC4469646.
53. Flynn M, Heale KA, Alisaraie L. Mechanism of Off-Target Interactions and Toxicity of Tamoxifen and Its Metabolites. *Chem Res Toxicol*. 2017; 30(7):1492–507. Epub 2017/06/14. <https://doi.org/10.1021/acs.chemrestox.7b00112> PMID: 28564538.
54. Manna S, Holz MK. Tamoxifen Action in ER-Negative Breast Cancer. *Sign Transduct Insights*. 2016; 5:1–7. <https://doi.org/10.4137/STI.S29901> PMID: 26989346; PubMed Central PMCID: PMC4792287.
55. DuSell CD, Nelson ER, Wittmann BM, Fretz JA, Kazmin D, Thomas RS, et al. Regulation of aryl hydrocarbon receptor function by selective estrogen receptor modulators. *Mol Endocrinol*. 2010; 24(1):33–46. Epub 2009/11/09. <https://doi.org/10.1210/me.2009-0339> PMID: 19901195; PubMed Central PMCID: PMC2802893.
56. Holleran AL, Lindenthal B, Aldaghlis TA, Kelleher JK. Effect of tamoxifen on cholesterol synthesis in HepG2 cells and cultured rat hepatocytes. *Metabolism*. 1998; 47(12):1504–13. [https://doi.org/10.1016/s0026-0495\(98\)90078-6](https://doi.org/10.1016/s0026-0495(98)90078-6) PMID: 9867082.
57. Gylling H, Pyrhönen S, Mäntylä E, Mäenpää H, Kangas L, Miettinen TA. Tamoxifen and toremifene lower serum cholesterol by inhibition of delta 8-cholesterol conversion to lathosterol in women with breast cancer. *J Clin Oncol*. 1995; 13(12):2900–5. <https://doi.org/10.1200/JCO.1995.13.12.2900> PMID: 8523053.
58. Cho SY, Kim JH, Paik YK. Cholesterol biosynthesis from lanosterol: differential inhibition of sterol delta 8-isomerase and other lanosterol-converting enzymes by tamoxifen. *Mol Cells*. 1998; 8(2):233–9. PMID: 9638657.
59. Jeong J, McMahon AP. Cholesterol modification of Hedgehog family proteins. *J Clin Invest*. 2002; 110(5):591–6. <https://doi.org/10.1172/JCI16506> PMID: 12208857; PubMed Central PMCID: PMC151115.
60. Huang P, Zheng S, Wierbowski BM, Kim Y, Nedelcu D, Aravena L, et al. Structural Basis of Smoothened Activation in Hedgehog Signaling. *Cell*. 2018; 174(2):312-24.e16. Epub 2018/05/24. <https://doi.org/10.1016/j.cell.2018.04.029> PMID: 29804838; PubMed Central PMCID: PMC6046275.
61. Myers BR, Neahring L, Zhang Y, Roberts KJ, Beachy PA. Rapid, direct activity assays for Smoothened reveal Hedgehog pathway regulation by membrane cholesterol and extracellular sodium. *Proc Natl*

Acad Sci U S A. 2017; 114(52):E11141–E50. Epub 2017/12/11. <https://doi.org/10.1073/pnas.1717891115> PMID: 29229834; PubMed Central PMCID: PMC5748227.

62. Heyne GW, Melberg CG, Doroodchi P, Parins KF, Kietzman HW, Everson JL, et al. Definition of critical periods for Hedgehog pathway antagonist-induced holoprosencephaly, cleft lip, and cleft palate. *PLoS One*. 2015; 10(3):e0120517. <https://doi.org/10.1371/journal.pone.0120517> PMID: 25793997; PubMed Central PMCID: PMC4368540.
63. Shenefelt RE. Morphogenesis of malformations in hamsters caused by retinoic acid: relation to dose and stage at treatment. *Teratology*. 1972; 5(1):103–18. <https://doi.org/10.1002/tera.1420050115> PMID: 5014447.
64. Heyne GW, Plisch EH, Melberg CG, Sandgren EP, Peter JA, Lipinski RJ. A Simple and Reliable Method for Early Pregnancy Detection in Inbred Mice. *J Am Assoc Lab Anim Sci*. 2015; 54(4):368–71. doi: n/a. PMID: 26224435; PubMed Central PMCID: PMC4521569.